S1 Sy_2 AOD_{550} validation with SURFRAD

The Surface Radiation Budget Network (SURFRAD) was established in 1993 through the support of National Oceanic and Atmospheric Administration's (NOAA) Office Global Programs (https://www.esrl.noaa.gov/gmd/grad/surfrad/overview.html, last access 04.01.2022). The AOD is measured with the MultiFilter Rotating Shadowband Radiometer (MFRSR) and freely available. The MFRSR infers the solar beam intensity by making successive global and diffuse measurements and computing their difference. In this way it simulates measurements of a sun photometer. In processing the raw data, the cosine response of the instrument is accounted for, thus allowing for accurate calibration using the Langley method. MFRSR channels (nominally 415, 500, 614, 670 and 868nm) are calibrated using a linearized form of Beer's Law to produce Langley plots from which an extrapolation to zero path length represents the calibration, or what the instrument would measure at the top of the atmosphere. Therefore, absolute calibration of the channels is not necessary for the AOD application. The Angstrom exponent is computed with the AODs for the 500-nm and 868-nm channels.

However, a simple cloud screening - all AOD values greater than 2.0 are removed to rid the time series of obvious cloud signals (Augustine et al., 2005) - limits the usage of the current product.

The Surface Radiation Budget Network (SURFRAD) was established in 1993 through the support of National Oceanic and Atmospheric Administration's (NOAA) Office Global Programs (https://www.esrl.noaa.gov/gmd/grad/surfrad/overview.html, last access 04.01.2022). The AOD is measured with the MultiFilter Rotating Shadowband Radiometer (MFRSR) and freely available. The MFRSR infers the solar beam intensity by making successive global and diffuse measurements and computing their difference. In this way it simulates measurements of a sun photometer. In processing the raw data, the cosine response of the instrument is accounted for, thus allowing for accurate calibration using the Langley method. MFRSR channels (nominally 415, 500, 614, 670 and 868nm) are calibrated using a linearized form of Beer's Law to produce Langley plots from which an extrapolation to zero path length represents the calibration, or what the instrument would measure at the top of the atmosphere. Therefore, absolute calibration of the channels is not necessary for the AOD application. The Angstrom exponent is computed with the AODs for the 500-nm and 868-nm channels.

However, a simple cloud screening - all AOD values greater than 2.0 are removed to rid the time series of obvious cloud signals (Augustine et al., 2005) - limits the usage of the current product.

Numbers of SY_2 / SURFRAD AOD matchups for each SURFRAD station for the period 2020.01-2021.09 are shown in **Error! Reference source not found.** for S3A. In total, for the study period, we have 985 matchups for S3A (971 matchups for S3B). We also show the location and number of matchups for the AERONET stations in the corresponding area, which allows understanding of the importance of the contribution of the SY_2 / SURFRAD AOD matchups into validation results.

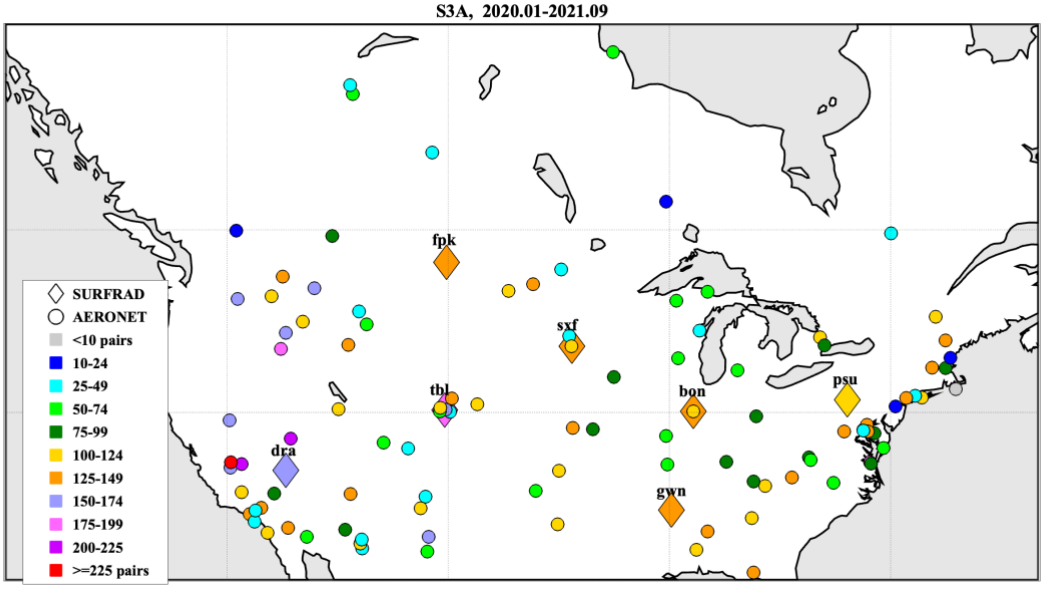

Figure S 1: Locations of SURFRAD ground-based stations (rhombus) used for S3A SY_2_AOD product validation and number (see legend) of matchups per stations for study period. AERONET stations (circles, coloured) are shown for reference.

A simple analysis of the agreement between SURFRAD and AERONET AOD measured at the stations which belong to different networks but located within 0.25° area was performed. Two stations fulfil this collocation criteria, BONDVILLE (bon) and Table Mountain (tbl). In general, the correlation between AOD measured by SURFRAD and AERONET is quite high (0.83-0.9), 73-83% of pairs fit to the strict EE defined with the GCOS requirements. However, few outliers are observed, when SURFRAD AOD is higher than AERONET AOD (Figure S3, supplement). The simple cloud screening for SURFRAD AOD can be a reason for those outliers.

Scatter plots with validation statistics for S3A and S3B for all, dual and singleN groups of SY_2/SURFRAD AOD matchups are shown in Figure S 2. The same tendency as in validation with AERONET exists, in that AOD is overestimated at low AOD loading and underestimated at high AOD loading. However, for both instruments and all groups, validation statistics are worse compared to AERONET (Sect.6, main paper). For all pairs, R (0.49/0.56 for S3A/S3B) is slightly lower than with AERONET; 53.8% and 61.1% of pixels fit into the EE, for S3A and S3B, respectively and only 30/33.4% of matchups satisfy the GCOS requirements. Among all groups, validation statistics are slightly better for dual group of matchups. Validation statistics are slightly better for S3B.

Since some disagreement between SURFRAD and AERONET AOD was revealed (Figure S 3), thus we do not recommend combining SY_2 AOD validation results with AERONET and SURFRAD, but rather consider them separately.

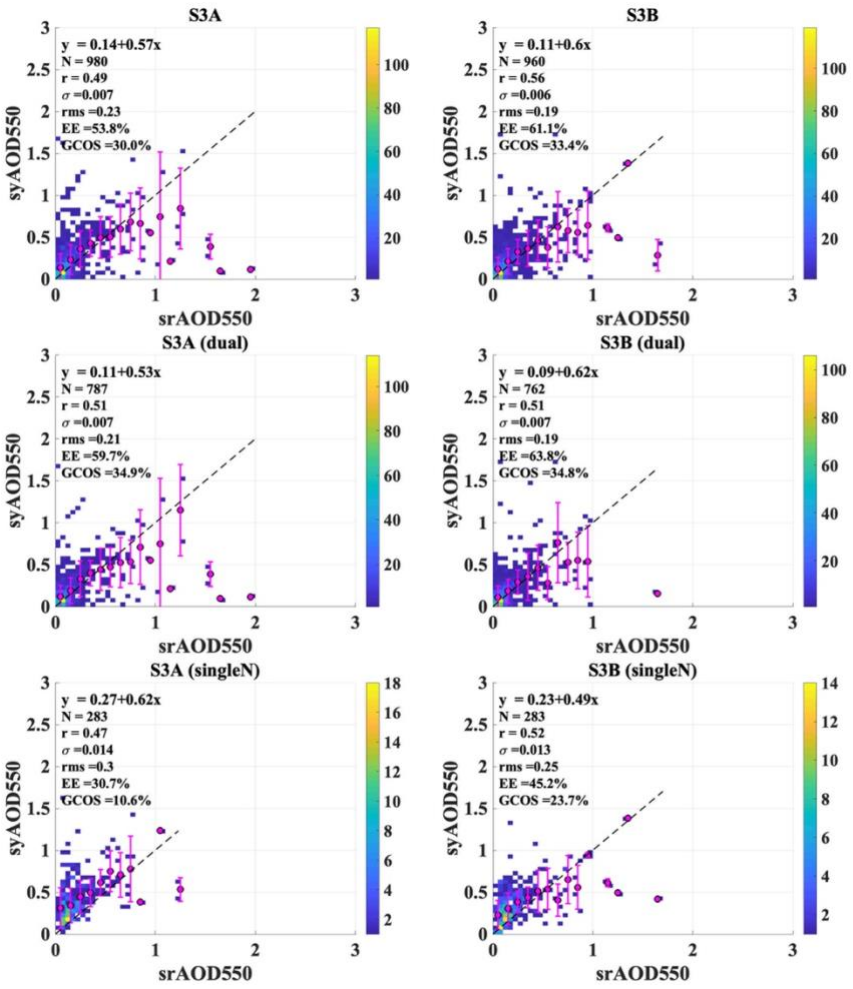

Figure S 2 : For S3A (left column) and S3B (right column), validation results for the whole product (upper panel), pixels retrieved with dual view processor (dual, middle panel), and single processor applied to the nadir view

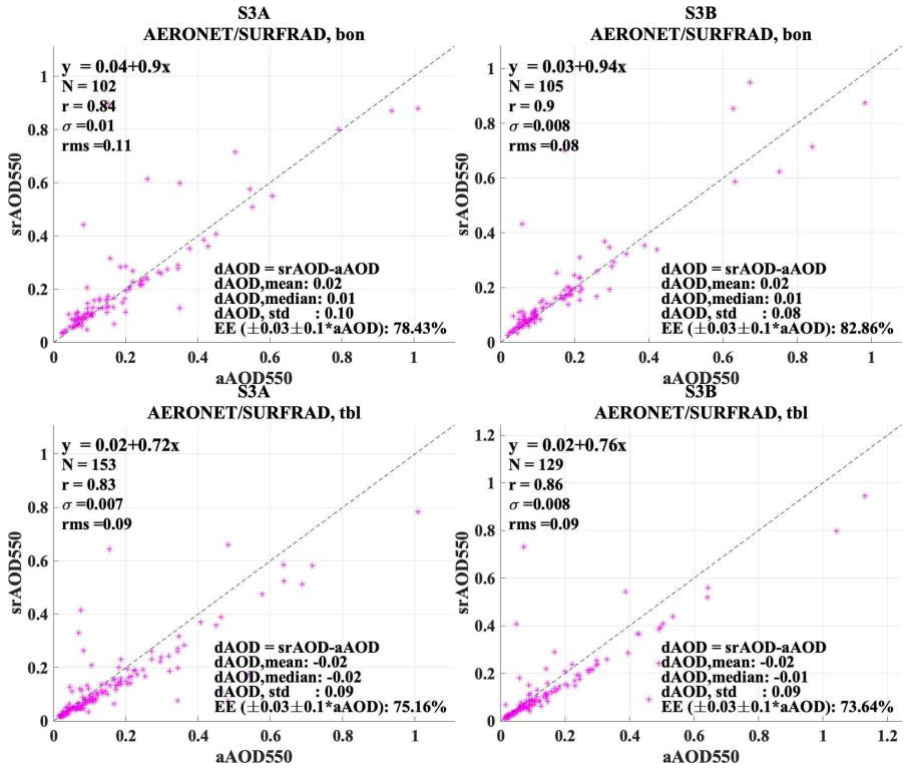

Figure S 3: Scatter plots for AOD measured at BON-SURFRAD and BONDVILLE-AERONET (upper panel), TBL-SURFRAD and Table Mountain-AERONET (lower panel) for S3A and S3B collocations (left and right panels, respectively)

S2 syAOD$_{550}$ validation with SKYNET

The SKYNET is a ground-based radiation observation network dedicated to aerosol-cloud-solar radiation interaction research (Takemura and Nakajima, 2004). SKYNET sites are located mostly in Europe, Japan and Thailand (https://www.skynet-isdc.org/obs_sites.php, last access 04.01.2022).

The standard instrument of each SKYNET sites is the sun-sky radiometer Prede Co. Ltd. model POM. The sun-sky radiometer is a scanning spectral radiometer able to perform routine and long-term automated measurements of direct and scattered solar radiations at seven wavelengths from 315 to 1020 nm (model POM-01) or eleven wavelengths from 315 to 2200 nm (model POM-02).

AOD is provided at the following wavelengths: 340, 380, 400, 500, 675, 870, 1020 nm. In general, SKYNET AOD compares well with AERONET AOD for any aerosol burden situation (Estelles et al., 2012, Hashimoto et al., 2012).

SKYNET aerosol products are available in near-real time for on-line sites and regularly for off-line sites.

Locations of the SKYNET stations included in current analysis and numbers of SY_2 / SKYNET AOD matchups for each SKYNET station (for S3A) are shown in Figure S 4. For S3B, number of pairs is similar.

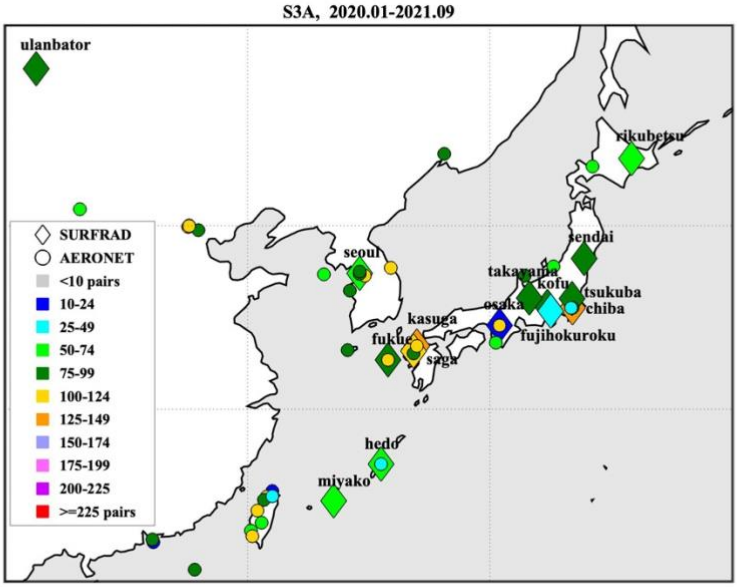

Figure S 4: Locations of SKYNET ground-based stations (rhombus) and numbers of S3A/SKYNET collocations are shown for each station with different colours (see legend). AERONET stations (circles, coloured) are shown for reference.

Intercomparison between SKYNET AOD and AERONET AOD was performed. For SKYNET stations which are located within 0.25° from the closest AERONET stations, scatter plots and validation statistics between SKYNET and AERONET AOD are shown in Figure S 5. The correlation coefficient is quite high (>0.78) for most of the stations, except for Osaka, where number of collocated points is low (N=14). However, few positive outliers are observed at each station. A positive AOD offset (snAOD>aAOD) of 0.13 is observed for Hedo (N=19). The existing offset between SKYNET and AERONET revealed in the current analysis is a reason to consider validation with AERONET and validation with SKYNET as separate exercises.

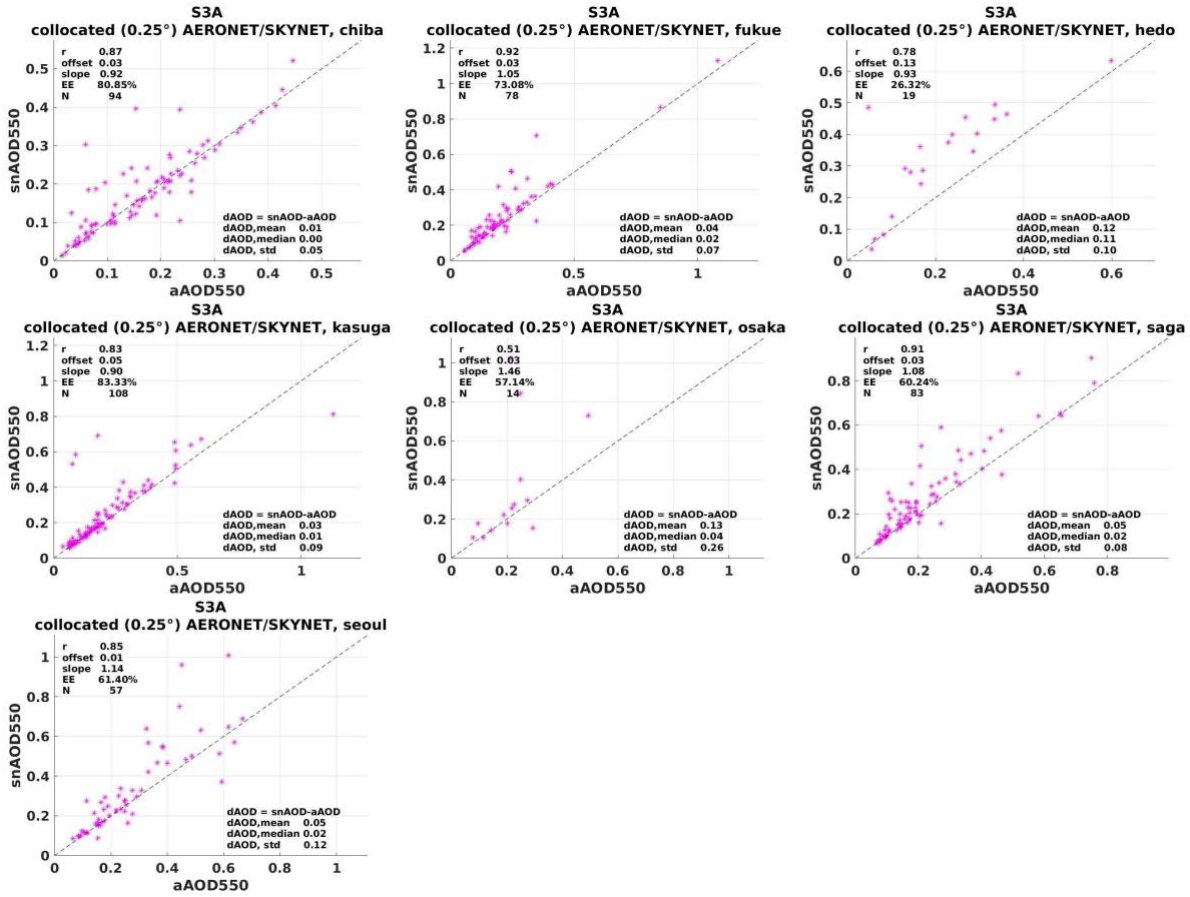

Figure S 5: Scatter plots for AOD measured at SKYNET (snAOD) and closely (less than 0.25° distance) located AERONET (aAOD) stations

Density scatter plots with validation statistics for S3A and S3B for all, dual and singleN groups of SY_2/SKYNET AOD matchups are shown in Figure S 6. The same tendency as in validation with AERONET exists, when SY_2 AOD is overestimated at low AOD and underestimated at high AOD. For both S3A and S3B and all groups, validation statistics are similar compared to AERONET (Sect.6, paper). For S3B, correlation coefficient R is slightly higher than for S3A (0.61 vs 0.57, for group 'all'), the number of points in EE for S3B is higher than for S3A (54.2% vs 43.7%, for group 'all'). Offset is higher for the group singleN.

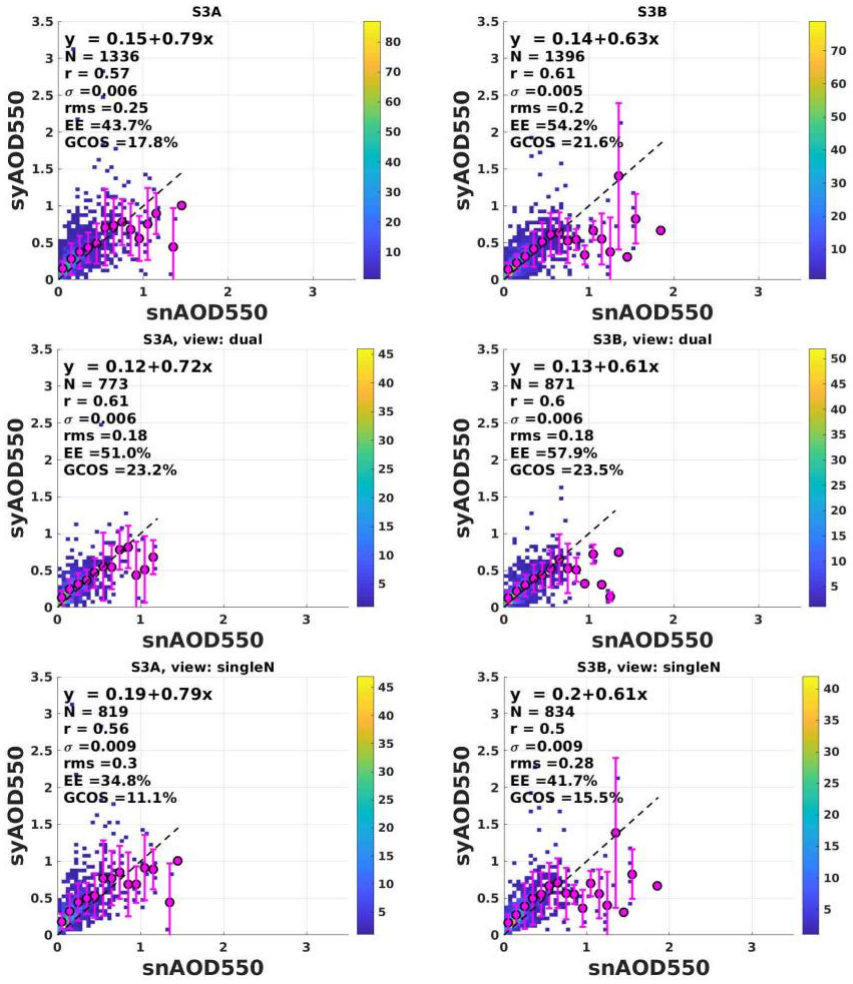

Figure S 6: For S3A (left column) and S3B (right column), validation results for the whole product (upper panel), pixels retrieved with dual view processor (dual, middle panel), and single processor applied to the nadir view (singleN, lower panel).

FIGURES

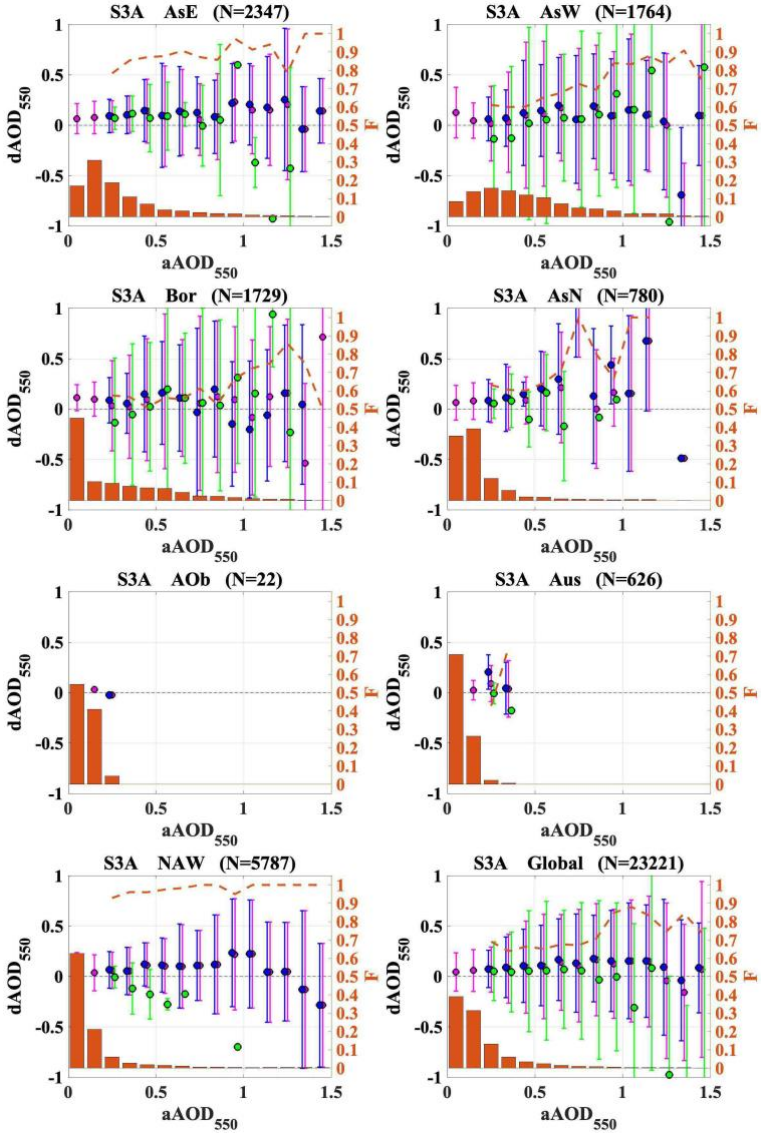

Figure S 7: As Fig. 7 in the main paper, regional (for AsW, AsE, AsN, Bor, AOb, Aus, NaW) and global difference ($dAOD_{550}$) between syAOD and aAOD for selected aAOD bins: median bias (circles) and bias standard deviation (error bars) for all and background (aAOD ≤ 0.2) AOD types (purple), aerosol fine-dominated AOD (blue) and coarse-dominated AOD (green). The fraction (F) of points in each bin from the total number of matchups is represented by orange bars.

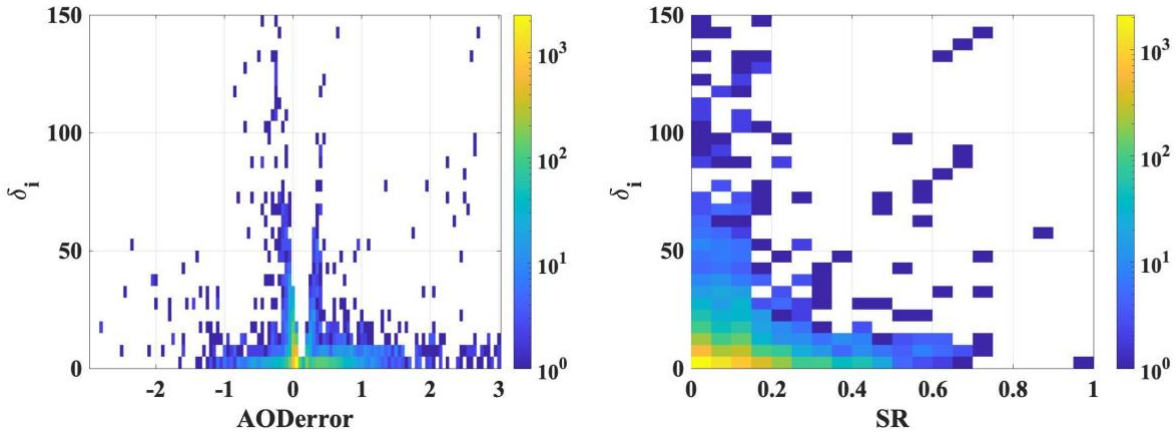

Figure S 8: Density scatter plot for individual weighted deviation for the goodness of PU and AODerror (left) and surface reflectance (right)

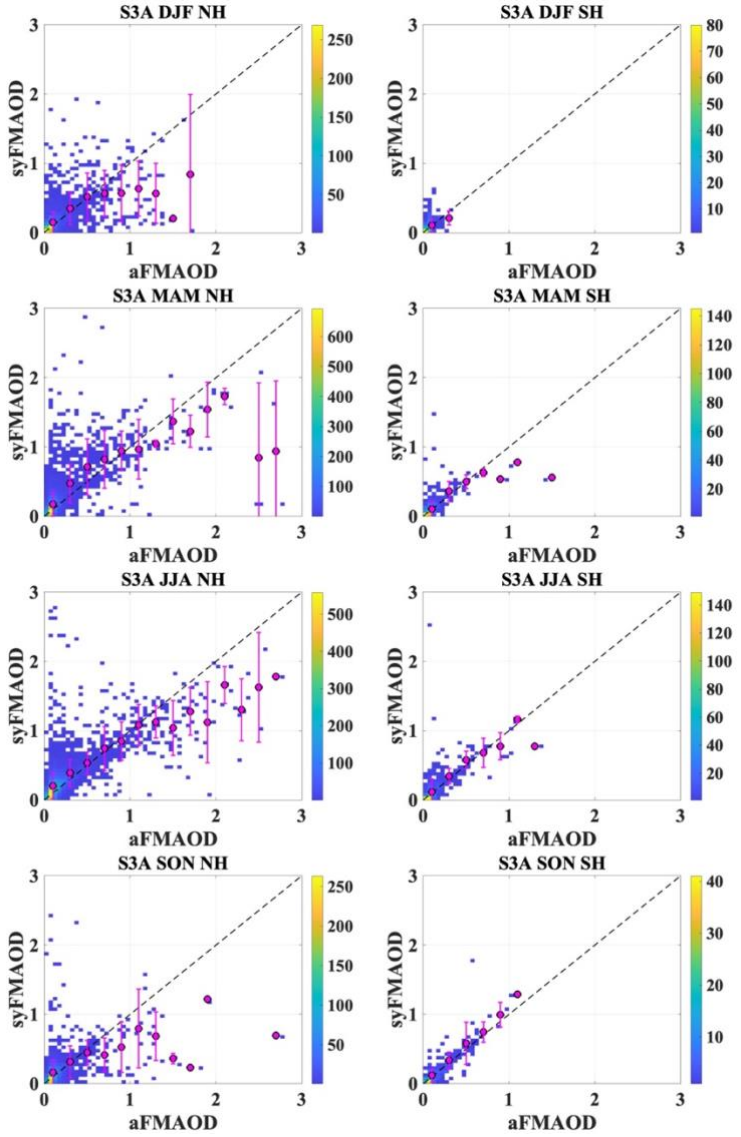

Figure S 9: Seasonal scatter density plots for S3A syFMAOD and corresponding aFMAOD for collocations available over the NH (left) and SH (right).

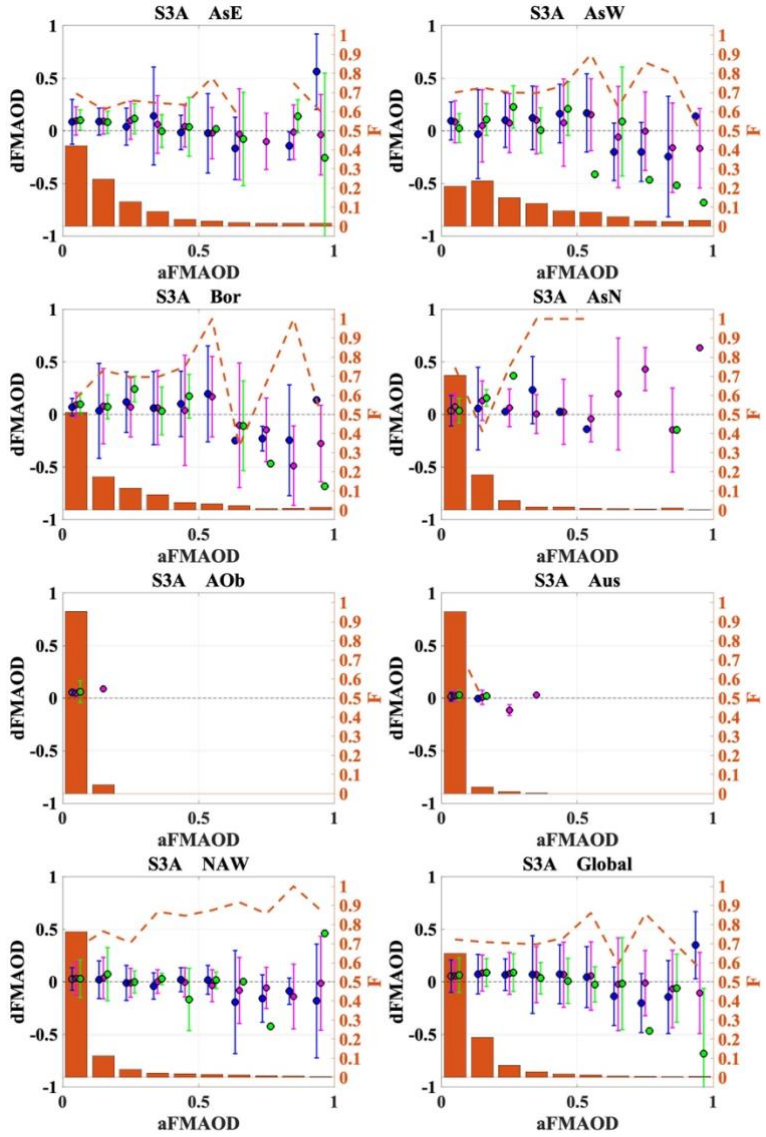

Figure S 10: As in Fig.19 main paper, regional (for AsW, AsE, AsN, Bor, AOb, Aus, NaW) and global difference (dFMAOD) between syFMAOD and aFMAOD for selected aFMAOD bins: median bias (circles) and bias standard deviation (error bars) for all AOD types (purple), aerosol fine-dominated AOD (blue) and coarse-dominated AOD (green). The fraction (F) of points in each bin from the total number of matchups is represented by orange bars. The fraction of fine-dominated matchups in each bin is shown as orange dashed-line.

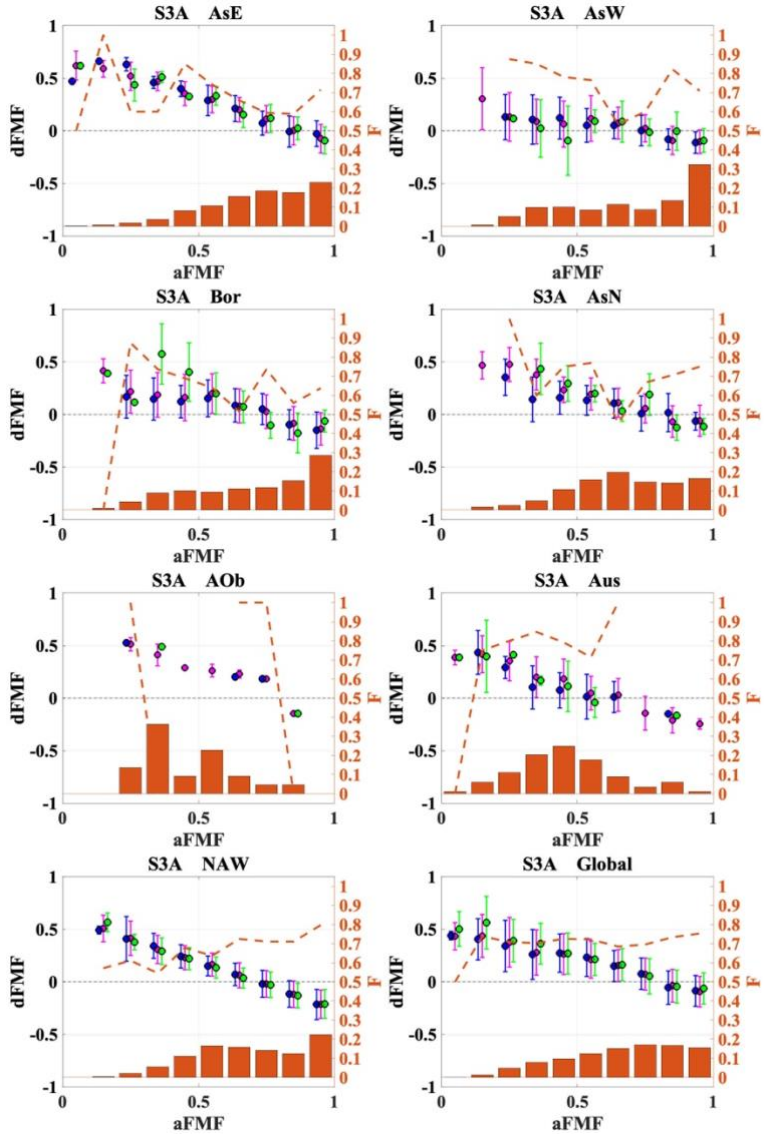

Figure S 11: As in Fig.22 main paper, regional (for AsW, AsE, AsN, Bor, AOb, Aus, NaW) and global difference (dFMF) between syFMF and aFMF for selected aFMF bins: median bias (circles) and bias standard deviation (error bars) for all AOD types (purple), aerosol fine-dominated AOD (blue) and coarse-dominated AOD (green). The fraction (F) of points in each bin from the total number of matchups is represented by orange bars. The fraction of fine-dominated matchups in each bin is shown as orange dashed-line.

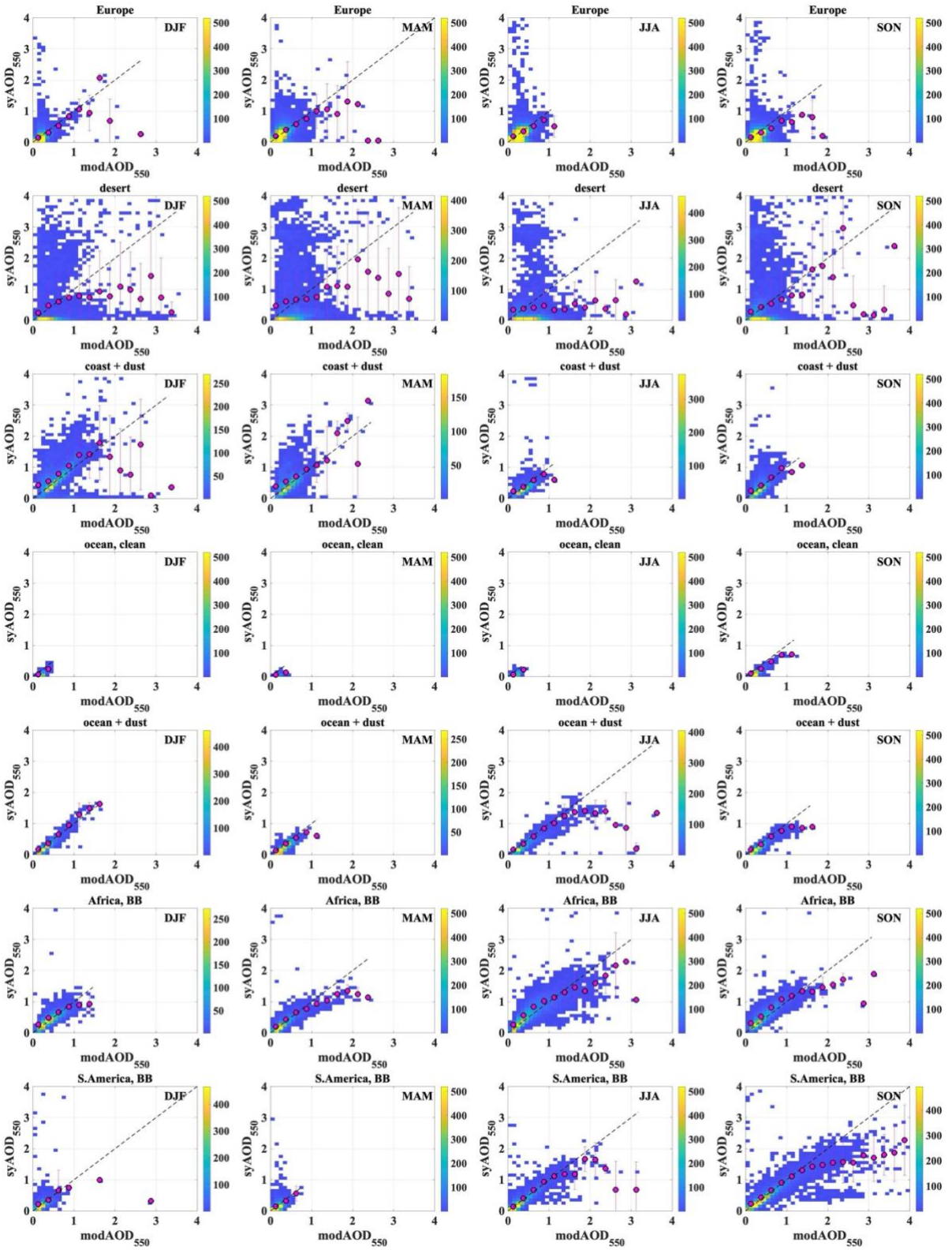

Figure S 12: Seasonal scatter density plots for MODIS Terra and S3A SY_2_AOD L3 daily collocated products for chosen sub-regions (as in top right corner)

TABLES

Table S1: Names and description of the aerosol properties retrieved

Name	Description
AOD440	Aerosol optical depth at 442.5nm
AOD550	Aerosol optical depth at 550nm
AOD670	Aerosol optical depth at 659nm
AOD865	Aerosol optical depth at 865nm
AOD1600	Aerosol optical depth at 1610nm
AOD440_uncertainty	Uncertainty of aerosol optical depth at 442.5nm
AOD550_uncertainty	Uncertainty of aerosol optical depth at 550nm
AOD670_uncertainty	Uncertainty of aerosol optical depth at 659nm
AOD865_uncertainty	Uncertainty of aerosol optical depth at 865nm
AOD1600_uncertainty	Uncertainty of aerosol optical depth at 1610nm
SSA440	Aerosol single scattering albedo at 442.5nm
SSA550	Aerosol single scattering albedo at 550nm
SSA670	Aerosol single scattering albedo at 659nm
SSA865	Aerosol single scattering albedo at 865nm
SSA1600	Aerosol single scattering albedo at 1610nm
AAOD550	Aerosol absorption optical depth at 550nm
FM_AOD550	Fine-mode aerosol optical depth at 550nm
ANG550_865	Aerosol Angstrøm parameter between 550nm and 865nm
D_AOD550	Dust aerosol optical depth at 550nm

Table S2: Definition of the sub-regions in the satellite AOD inter-comparison exercise.

Sub-region	Properties	Short name, as on figures	Location
Europe	highly populated with possible anthropogenic emissions	Europe	36°N-60°N, 10°E-45°E
Sahara Desert	bright surface, dust aerosols	desert	10°N-30°N, 10°W-20°E
South Africa	seasonal biomass burning	S.Africa, BB	15°S-5°N, 30°W-15°W
South America	seasonal biomass burning	S.America, BB	20°S-0°N, 50°W-70°W
Atlantic Ocean	possible dust outbreaks over ocean	ocean+dust	10°N-30°N, 17°W-30°W
coastal area	land/ocean transition zone, possible dust outbreaks	coast+dust	0°N-10°N, 20°W-10°E
clean ocean	marine aerosols, possibly clean air	ocean, clean	30°S-20°S, 30°W-10°W

Table S3: Evaluation statistics for the agreement in daily AOD of 1°x1° resolution between S3A SY_2 and MODIS Terra AOD550 for sub-regions defined in Table S1.

area	period	R	rms	sigma	bias	slope	N
coast + dust		0,62	0,34	0,003	0,14	0,95	13810
	DJF	0,55	0,46	0,006	0,29	0,81	4596
	MAM	0,48	0,38	0,007	0,24	0,81	2374
	JJA	0,51	0,22	0,005	0,07	0,84	2191
	SON	0,58	0,21	0,003	0,07	1,01	4649
desert		0,18	0,77	0,005	0,27	0,39	28547
	DJF	0,22	0,78	0,009	0,24	0,41	7181
	MAM	0,14	0,94	0,013	0,46	0,32	5602
	JJA	0,05	0,73	0,009	0,33	0,11	6115
	SON	0,21	0,69	0,007	0,22	0,53	9649
Africa, BB		0,84	0,23	0,001	0,16	0,89	23104
	DJF	0,78	0,17	0,003	0,16	0,81	3477
	MAM	0,81	0,16	0,002	0,1	0,81	4968
	JJA	0,83	0,28	0,003	0,22	0,83	8810
	SON	0,87	0,22	0,002	0,18	0,96	5849
ocean + dust		0,89	0,11	0,001	0,03	0,86	10800
	DJF	0,95	0,08	0,001	-0,02	1,12	2516
	MAM	0,9	0,08	0,002	-0,03	1,04	2230
	JJA	0,87	0,19	0,004	0,08	0,75	2317
	SON	0,92	0,06	0,001	0,02	0,9	3737
ocean, clean		0,88	0,04	0	0	0,72	15583
	DJF	0,8	0,04	0,001	0	0,67	3527
	MAM	0,63	0,04	0,001	0,02	0,47	2281
	JJA	0,83	0,03	0	0,01	0,67	6206
	SON	0,9	0,05	0,001	0	0,77	3569
S.America, BB		0,87	0,2	0,001	0,1	0,78	29096
	DJF	0,31	0,23	0,004	0,17	0,41	2789
	MAM	0,55	0,11	0,001	0,05	0,85	5674
	JJA	0,89	0,12	0,001	0,06	0,92	11738
	SON	0,85	0,29	0,003	0,19	0,69	8895
Europe		0,54	0,15	0	0,07	0,8	127169
	DJF	0,49	0,13	0,001	0,06	0,78	15908
	MAM	0,53	0,18	0,001	0,1	0,8	23532
	JJA	0,53	0,15	0,001	0,08	0,82	46659
	SON	0,53	0,14	0,001	0,06	0,74	41070
AOI		0,46	0,3	0	0,07	0,76	909963
	DJF	0,42	0,33	0,001	0,06	0,86	168277
	MAM	0,39	0,32	0,001	0,07	0,72	190489
	JJA	0,51	0,27	0,001	0,06	0,73	277707
	SON	0,49	0,3	0,001	0,07	0,79	273490

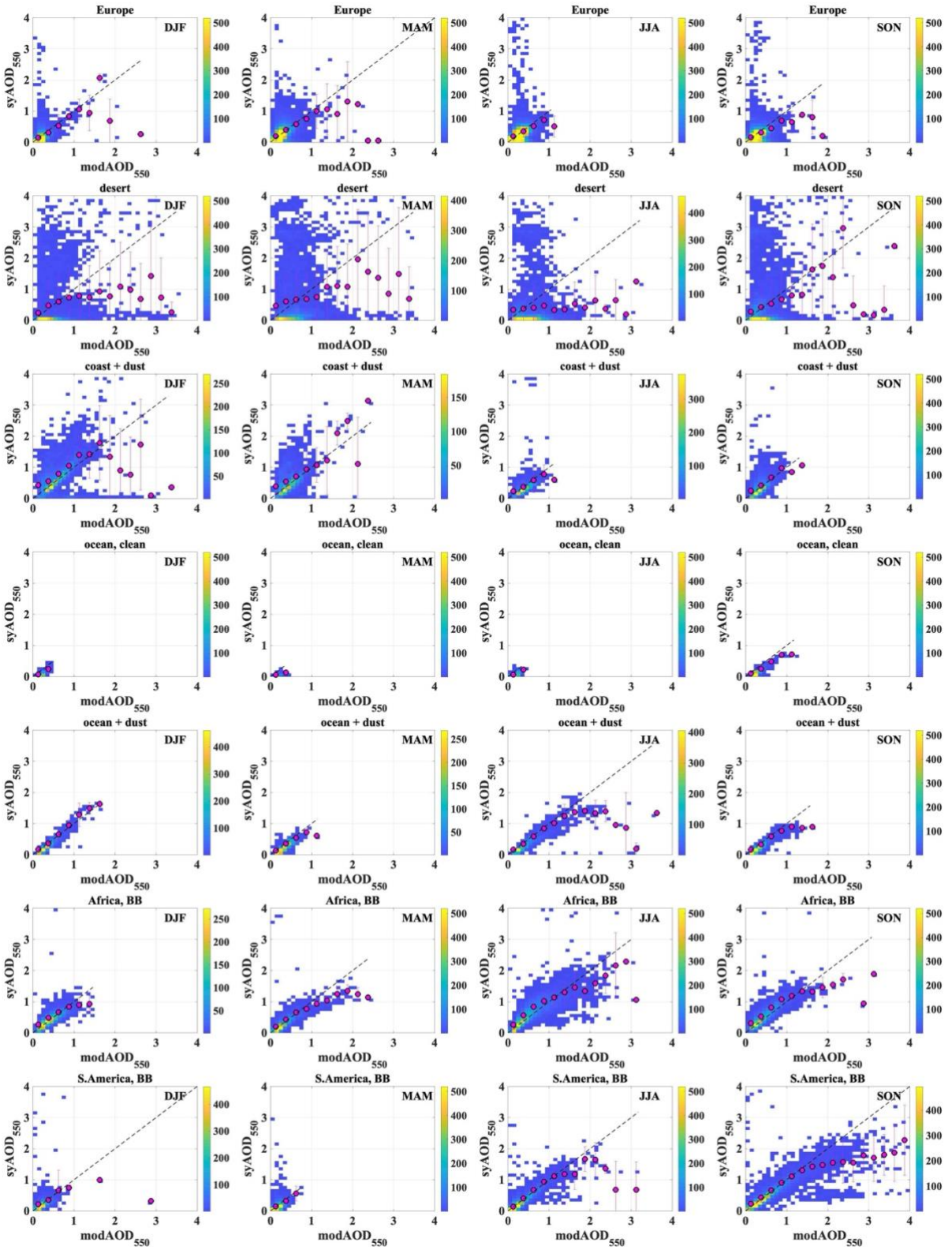

Figure S5 Seasonal scatter density plots for MODIS Terra and S3A SY_2_AOD L3 daily collocated products for chosen sub-regions (as in top right corner)

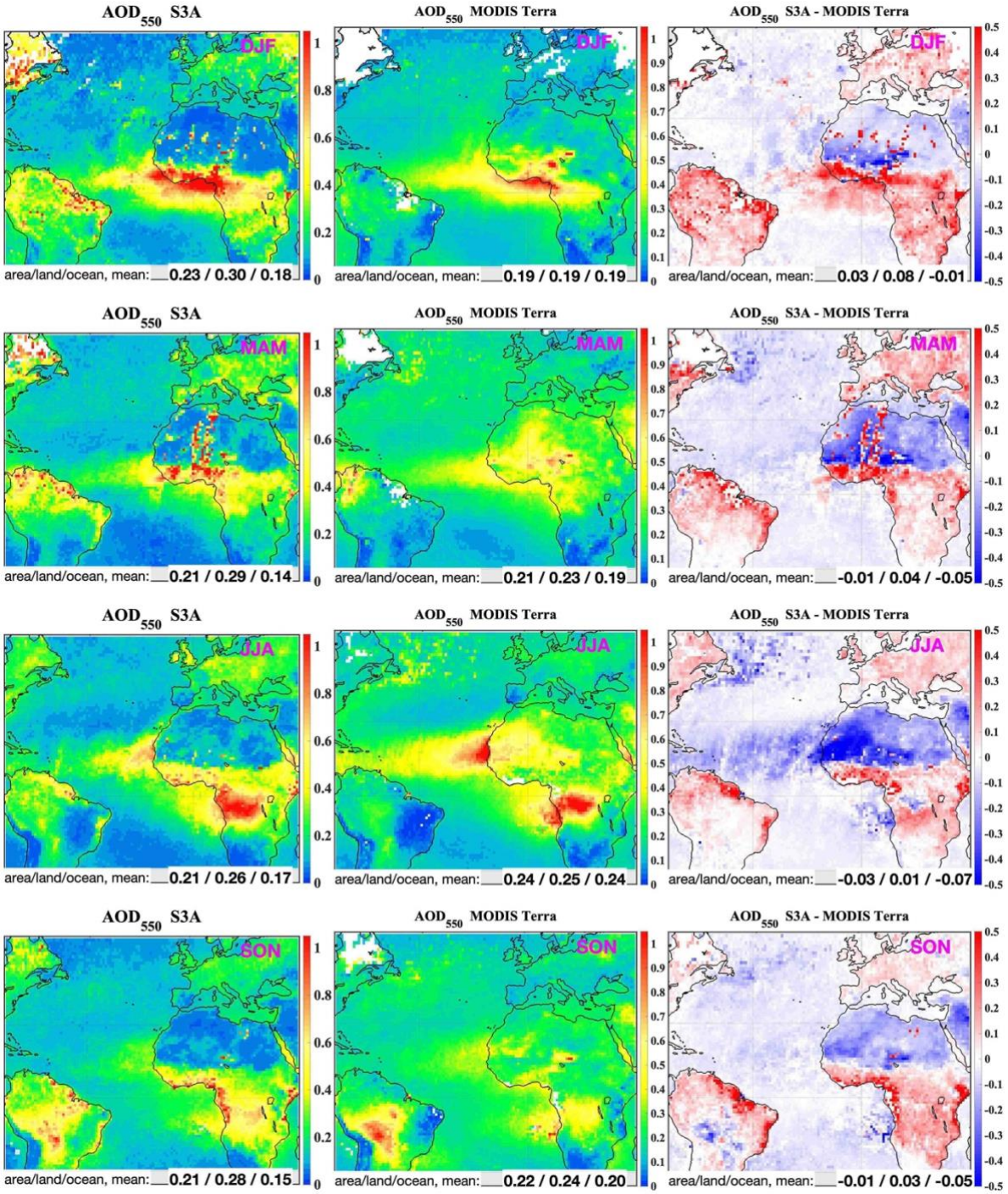

Figure S6: Seasonal (top down: DJF, MAM, JJA, SON) S3A (left panel), MODIS Terra (middle panel) AOD and difference in AOD between S3A and MODIS Terra (right panel). From monthly aggregates created from all available data in S3A and MODIS Terra daily AOD products.